UTRIP: Project Report

Tsunami Interferometry: Detecting the Kuroshio Current

Tarak Yadav[1]

[1]IISER Kolkata

Under the guidance of Prof. Shingo Watada, ERI

Abstract

In this project, we discuss tsunami interferometry, a novel technique used in extracting virtual tsunami waves between a pair of ocean-bottom pressure stations. We discuss the theory of the technique, the details of signal processing and the extraction of meaningful results from the processed data.

Keywords: **Tsunami, Interferometry, Cross-correlation**

September 17, 2024

1 Introduction

Ocean currents, abiotic features of the environment, are continuous and directed movements of ocean water. These currents are on the ocean's surface and in its depths, flowing both locally and globally.[1]

For this project, we focus on the Kuroshio Current, a north-flowing, warm ocean current on the west side of the North Pacific Ocean basin (Figure 1). It brings warm subtropical waters from the Indo-Pacific Warm Pool to Japan, exerting a major control on the Asian climate.

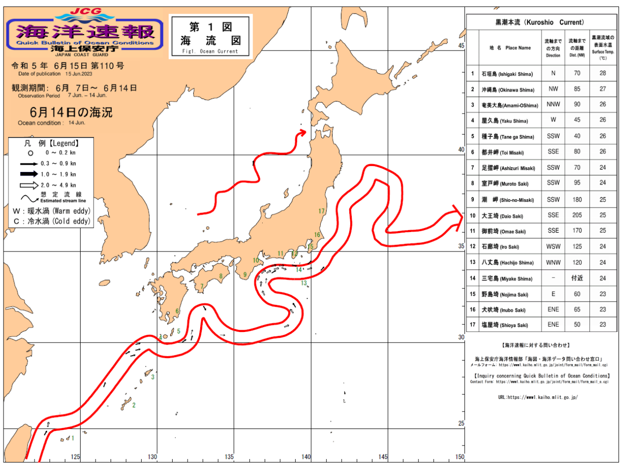

Figure 1: The Kuroshio Current in June 2023[2]

2 Ambient Noise Tomography

Commonly used in seismology, ambient noise tomography uses the cross-correlation of diffuse wavefields to estimate the Green function between stations. The stations act as virtual sources for each other, giving us a dispersed waveform from which surface wave speeds can be measured.

Figure 2 illustrates how the noise sources distributed in 2D around the pair of stations contribute to the cross-correlated waveforms between the records at the two stations. The noise source S' lies in the coherency zone (grey) and contributes to virtual waves between A and B. A source that lies outside the coherency zone, like S, does not contribute to virtual waves between A and B.

Explanation: Cross-correlation corresponds to taking the time difference of the signals that are analyzed; hence, the noise generated by source S gives, after cross-correlation, a wave arriving at time $t_{SA} - t_{SB}$. In general, $t_{SA} - t_{SB} \neq t_{AB}$, so the contribution of source S does not correspond to a wave propagating between the receivers.[9]

3 Tsunamis

- Tsunamis are usually generated due to submarine landslides and earthquakes.
- Long-period tsunami waves also exist in the ambient noise that is observed in ocean bot-

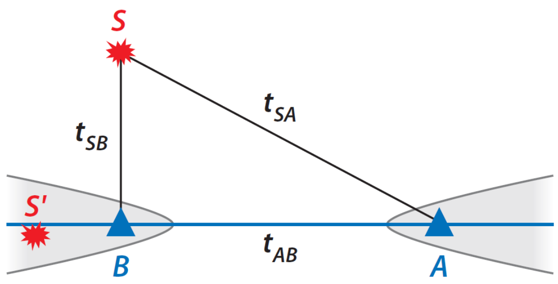

Figure 2: Receivers A and B and noise sources S and S'.[9]

tom pressure records. We focus on these records.

- Virtual tsunami waves are extracted between a pair of stations for this project.

3.1 Dispersion

A dispersive wave can be modelled by the dispersion relation:[8]

$$u(x,t) = \Delta\omega \left(\frac{\sin Y}{Y}\right) \cos\left(\omega_0 - k(\omega_0)x\right) \quad (1)$$

$$Y = \left(\frac{\Delta\omega}{2}\right)\left(t - \left(\frac{dk}{d\omega}\right)_{\omega_0} x\right) \quad (2)$$

The wave envelope propagates with a group velocity, U, while the phase of the wave propagates with the phase velocity c. The two are related as follows:

$$U = \frac{d\omega}{dk} = c - \Lambda\frac{dc}{d\Lambda} \quad (3)$$

3.2 Calculating Phase Velocity

The phase of a particular frequency can be expressed as:

$$\phi(\omega) = \phi_0(\omega) - \frac{\omega x}{c(\omega)} + 2\pi N + \omega t \quad (4)$$

Here, $\phi_0(\omega)$ is the initial phase at the source, x is the distance from the source, t is the time after origin time and $2\pi N$ corresponds to the phase ambiguity due to the periodicity of the harmonic function.
Repeating the phase measurement for two stations, we obtain the following relation for the phase velocity:

$$c(\omega) = \frac{x_1 - x_2}{(t_1 - t_2) + T\left(M - \frac{1}{2\pi}(\phi_1(\omega) - \phi_2(\omega)\right)} \quad (5)$$

3.3 Dispersive Tsunami Model

The dispersion relation for a linear surface gravity wave propagating through an ocean with depth D can be modelled by the equation:[10]

$$\frac{\omega}{k} = \sqrt{\frac{g}{k}\tanh kD} \quad (6)$$

Here, g is the acceleration due to gravity. This relation has been used to plot the dispersive tsunami model in the results. In equation 6, effects of the elastic ocean, compressible Earth, and gravity potential change have not been accounted for in Figure 3 as various tsunami dispersion models.

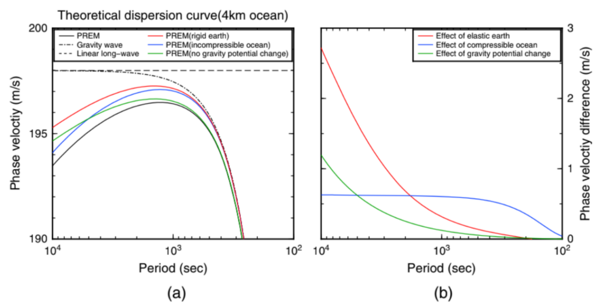

Figure 3: Dispersion relations of the tsunami phase velocity for various models: *Watada et al. (2014)*

4 Mathematical Prerequisites

4.1 Cross-correlation

The cross-correlation for two continuous functions f and g is defined as:[7]

$$(f \star g)(\tau) = \int_{-\infty}^{\infty} \overline{f(t)}g(t+\tau)dt \quad (7)$$

The cross-correlation between two discrete time sequences a_n and b_n of lengths N and M respectively is defined as:[7]

$$c_k = \frac{1}{N+M-1}\sum_p a_p b_{p+k} \quad (8)$$

Cross-correlation can be described as a measure of the similarity of two series as a function of the displacement of one relative to the other.

4.2 Fourier Transform

The Discrete Fourier Transform (DFT) of a time sequence a_k is given by the transformation equation:

$$A_n = \frac{1}{N}\sum_{k=0}^{N-1} a_k e^{-2\pi ink/N} \tag{9}$$

Here A_n's are the Fourier coefficients, and $1/N$ is used as a normalising factor.
Similarly, the Inverse Discrete Fourier Transform of the sequence A_n is given by the transformation equation:

$$a_k = \sum_{n=0}^{N-1} A_n e^{2\pi ink/N} \tag{10}$$

The Fourier coefficient can be expressed as:
$A_n = R_n e^{i\phi_n}$ where R_n (real part) is the maximum value of the sine wave and ϕ_n is the phase of the frequency.

4.3 Properties of the DFT[7]

1. **Time Reversal:** For a time-reversed sequence $a'_k = a_{N-k}$, we can make the substitution $l = N - k$ to obtain:

$$\begin{aligned} A'_n &= \frac{1}{N}\sum_{k=0}^{N-1} a_{N-k} e^{-2\pi ink/N} \\ &= \frac{1}{N}\sum_{l=0}^{N-1} a_l e^{-2\pi in(N-l)/N} = A_n^* \end{aligned}$$

   This means that the time reversal of the sequence complex conjugates the DFT.

2. **Periodic repetition:**

$$a_{k+N} = a_k \tag{11}$$

$$A_{n+N} = A_n \tag{12}$$

3. **Parseval's Theorem:** Equality of "energy" between time and frequency domains:

$$|A_n|^2 = \frac{1}{N^2}\sum_{k=0}^{N-1} a_k e^{-2\pi ink/N} \sum_{l=0}^{N-1} a_l e^{2\pi inl/N}$$

$$\begin{aligned} \sum_{n=0}^{N-1} |A_n|^2 &= \frac{1}{N^2}\sum_{k,l} a_k a_l \sum_{n=0}^{N-1} e^{-2\pi in(k-l)/N} \\ &= \frac{1}{N}\sum_{k,l} a_k a_l \delta_{kl} \\ &= \frac{1}{N}\sum_{k=0}^{N-1} |a_k|^2 \end{aligned}$$

4.4 Fast Fourier Transform

FFT is a commonly used algorithm which reduces the number of numerical operations of the Fourier transform and speeds up computation:

$$\begin{aligned} NA_n &= \sum_{k=0}^{N-1} a_k e^{-2\pi ink/N} \\ &= \sum_{k=0}^{N/2-1} a_k e^{-2\pi ink/N} + \sum_{k=N/2}^{N-1} a_k e^{-2\pi ink/N} \\ &= \sum_{k=0}^{N/2-1} (a_k + a_{k+N/2} e^{-\pi in}) e^{-2\pi ink/N} \end{aligned}$$

The total number of operations has reduced from N^2 to $(\frac{N^2}{2} + \frac{N}{2})$ which becomes a considerable reduction for large values of N.

4.5 Cross-correlation in Frequency Domain

Multiplication in the frequency domain corresponds to convolution in the time domain:

$$c = a * b \Longleftrightarrow C_n = A_n B_n \tag{13}$$

Using this and the time reversal property of the DFT, we can demonstrate the following for cross-correlation in the frequency domain:

$$c = a \star b \Longleftrightarrow C_n = A_n^* B_n \tag{14}$$

Hence, instead of cross-correlating two time sequences in the time domain, we can speed up computation by using the FFT to find the cross-correlation in the frequency domain and then Inverse Fourier Transforming the sequences to the time domain.

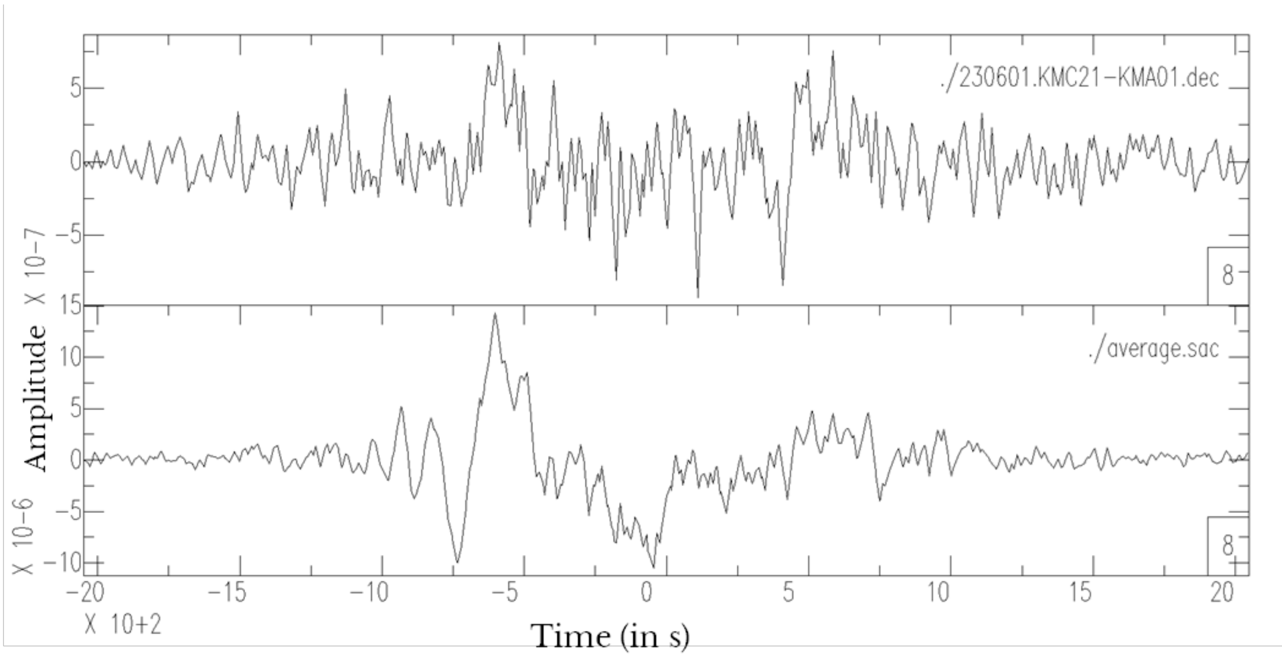

Figure 4: Cross-correlated waveforms (low-pass filtered: 0.02 Hz) for the station pair KMC21 - KMA01 for: 1st June 2023 (above) and the entire month of June 2023 stacked (below). Negative time lag indicates waves travelling from KMC21 to KMA01.

5 Processing Details

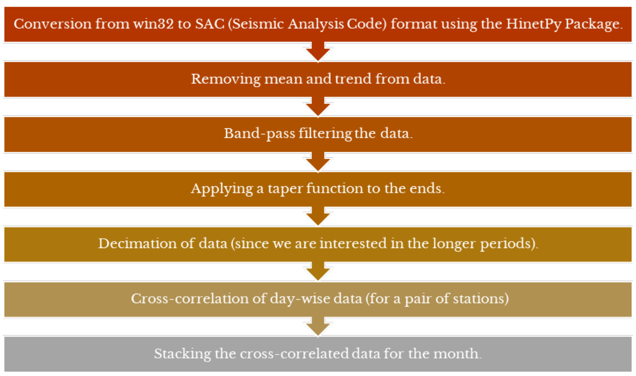

Figure 5: An overview of the processing details

5.1 Data Source

An ocean-floor observation network called DONET (Dense Oceanfloor Network system for Earthquakes and Tsunamis) was deployed in the Kumano Nada Sea and off the Kii Channel, which are the starting areas of destruction for huge earthquakes. The observation networks deployed in the Kumano Nada Sea and off the Kii Channel are called DONET1 and DONET2, respectively. DONET1 began full-scale operation with 20 observation points in July 2011, and DONET2 began full-scale operation in March 2016.[3]
Pressure data was taken from DONET stations off the coast of Japan for the month of June 2023.

Figure 6: DONET stations[3]

5.2 Data Conversion

Data obtained from DONET stations was in *win32* format. This was converted to *SAC* format using the *HinetPy* package in *python*. The data and channel table were used to convert day-wise data to *SAC* format using the *win32.extract_sac()* module.

5.3 Signal Processing, Cross-Correlation and Stacking

- *SAC* was used to remove mean and trend from the data (day-wise).
- The data was then bandpass filtered between the frequencies 0.001 and 0.06 Hz.
- A taper function was applied to the ends. Tapering refers to the process of obtaining a more favorable Fourier spectrum with a better central peak by smoothing the sharp edges in the window of data under consideration. This preserves more of the important information in a time series and reduces the effect of the edges.[7]
- The data was then decimated (decimation every 2 samples, followed by decimation every 5 samples = decimation every 10 samples).
- Day-long data for a pair of stations was cross-correlated according to Equation 14. The cross-correlation was performed after taking the FFT of the time sequence with adequate zero padding. The cross-correlated waveform was converted back to the time domain through an IFT.
- The positive lag part of the cross-correlation is sometimes called the 'causal' signal, and the negative lag part is the 'acausal' signal. These waveforms represent waves travelling in opposite directions between the stations (Figure 2).
- Cross-correlations were computed for the same pair of stations (day-wise) for a month, and these records were stacked (Figure 4).[5]

6 Results

Stations of interest were chosen after observing the prevailing conditions of the Kuroshio Current from the JMA (Japan Meteorological Agency) and Japan Coast Guard data for the month of June 2023 and overlaying it with a map of DONET stations.

1. A dispersed tsunami waveform can be seen after stacking cross-correlated records for an adequate amount of time.

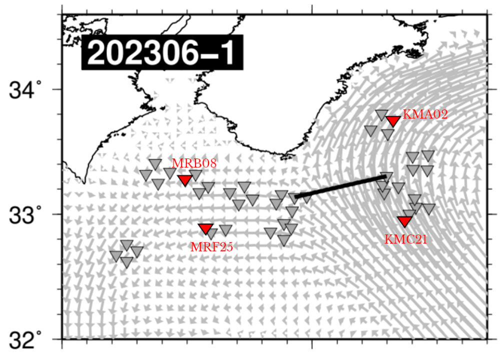

Figure 7: Stations of interest marked on a map with the Kuroshio Current[4]

2. The cross-correlation is stronger on one side since the ambient noise sources are not homogeneously distributed.
3. The amplitude spectrum (after a Fast Fourier transform) shows us that higher amplitudes are from longer periods.

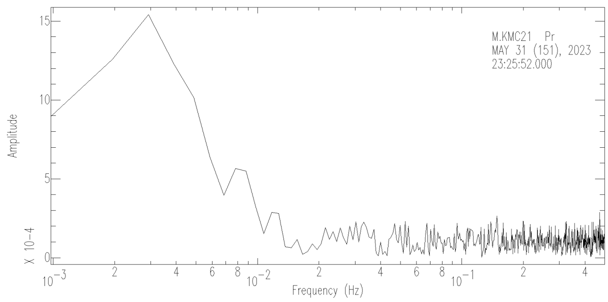

Figure 8: Amplitude spectrum obtained after a Fast Fourier Transform of the stacked cross-correlations between station KMC21 and KMA01 for June 2023

The phase velocity can be calculated using Equation 5. The phase ambiguity M is difficult to measure for shorter periods since tsunami waves are mostly long-period waves (as we saw in Figure 8).

The phase ambiguity can be resolved by using the existing equation, which approximates the non-dispersive tsunami wave speed for shallow depth, D, as:[8][6]

$$c_s = \sqrt{gD} \tag{15}$$

The phase velocity can then be found using the equation:[10]

$$c = c_s - \frac{\Delta\phi(x,\omega) - 2\pi M}{\omega x} c_s^2 \tag{16}$$

6.1 KMC21-KMA02

We found the cross-correlation between station pairs KMC21-KMA(01-04) and consistently observed a phase velocity difference of 3-10 m/s between the positive and negative parts of the cross-correlation in the long-period region (Figure 10).

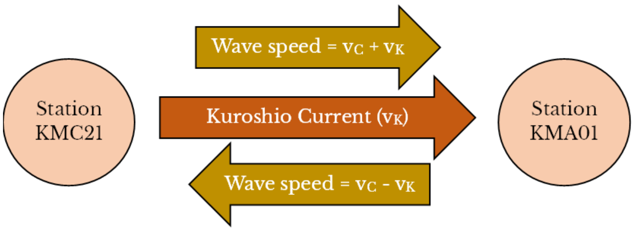

Figure 9: A schematic illustrating stations lying along the direction of the current

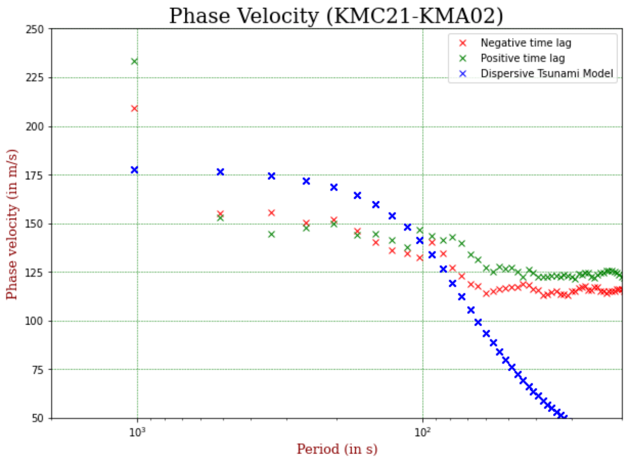

Figure 10: Phase velocity curves for cross-correlation between KMC21-KMA02

6.2 MRB08-MRF25

We found the cross-correlation between station pairs of DONET-2 and consistently observed negligible phase velocity differences between the positive and negative parts of the cross-correlation in the long-period region (Figure 12).

7 Conclusions

The maximum speed of the Kuroshio current is 4.9 knots (around 2.5 m/s), so the observed phase velocity difference for station pairs considered above in DONET-1 is consistent with the expected phase velocity difference of 5 m/s (due to the movement of the medium due to the Kuroshio current). We

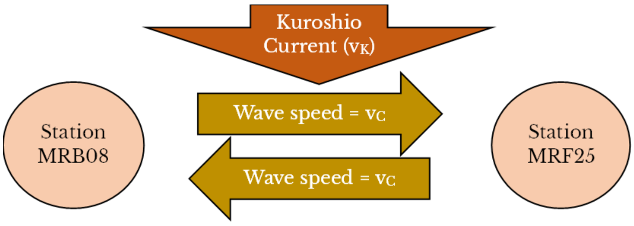

Figure 11: A schematic illustrating stations with the line joining them lying perpendicular to the direction of the current

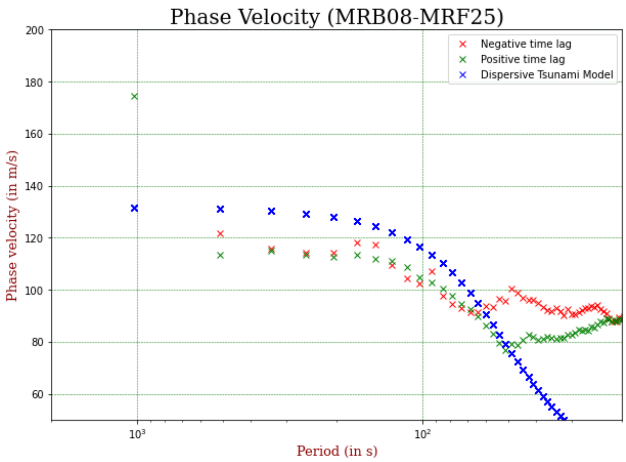

Figure 12: Phase velocity curves for cross-correlation between MRB08-MRF25

also do not expect any phase velocity difference for station pairs which lie such that the line joining them is perpendicular to the flow of the Kuroshio Current (as seen in many DONET-2 station pairs). Nevertheless, further work is needed to substantiate the claims.

8 Further Work

1. Better error estimation is needed to quantify the observations accurately.
2. S-net stations might provide better coverage to map the Kuroshio current as compared to DONET stations.
3. Longer records can be stacked so that a clear dispersed waveform can be observed in the cross-correlated record. However, the Kuroshio meander is constantly fluctuating over small periods of time, and this reduces the accuracy of phase velocity measurements.
4. Currently, the technique has scopes for error since it involves manual intervention to

pick the dispersed waveform (from the cross-correlated waveform).

5. Source inhomogeneity must be taken care of using SNR or other similar tests since most cross-correlated waveforms show a stronger cross-correlation on one side.

9 Acknowledgements

I would like to express my sincere gratitude to Prof. Shingo Watada for his unwavering support throughout the internship. The concepts that I learnt were truly unique and hold great importance in tsunami wave interferometry and ambient noise seismology. I learnt a lot about tsunami dynamics, too, which was a completely novel field for me.
I would also like to thank my UTRIP supporter, Morita-san, ERI and the UTRIP team for their constant help throughout the project (especially Jono-san for arranging vegan food during UTRIP events). This project was funded by the GSS-UTRIP scholarship.
Lastly, I would also like to acknowledge SAC, Python, HinetPy, DONET data and Gnuplot that were used for the internship.

References

[1] June 2024. NOAA: https://www.noaa.gov/.

[2] June 2024. Japan Coast Guard: https://www1.kaiho.mlit.go.jp.

[3] June 2024. DONET: https://www.seafloor.bosai.go.jp/DONET/.

[4] June 2024. JMA: https://www.data.jma.go.jp.

[5] G. D. Bensen, M. H. Ritzwoller, M. P. Barmin, A. L. Levshin, F. Lin, M. P. Moschetti, N. M. Shapiro, and Y. Yang. Processing seismic ambient noise data to obtain reliable broad-band surface wave dispersion measurements. *Geophysical Journal International*, 169(3):1239–1260, 06 2007.

[6] Someya et al. 2d fdm simulation of seismic waves and tsunamis based on improved coupling equations under gravity: Supplementary file 2. *Pure and Applied Geophysics*, 2024.

[7] David Gubbins. *Time Series Analysis and Inverse Theory for Geophysicists.*

[8] Lay and Wallace. *Modern Global Seismology.* Academic Press.

[9] Roel Snieder and Eric Larose. Extracting the earth response from noise measurements. May 2012.

[10] Shingo Watada, Satoshi Kusumoto, and Kenji Satake. Traveltime delay and initial phase reversal of distant tsunamis coupled with the self-gravitating elastic earth. *Journal of Geophysical Research: Solid Earth*, 119(5):4287–4310, 2014.